

Piece-wise transition detection algorithm for a self-mixing displacement sensor

Zhen Huang (黄 贞), Chengwei Li (李成伟), and Xiaogang Sun (孙晓刚)*

School of Electrical Engineering and Automation, Harbin Institute of Technology, Harbin 150001, China

*Corresponding author: sxg@hit.edu.cn

Received April 14, 2013; accepted June 28, 2013; posted online August 30, 2013

A piece-wise transition detection algorithm that performs displacement measurements for self-mixing sensors is developed. The algorithm can correctly detect self-mixing fringes at a low signal-to-noise ratio in the presence of disturbances without filtering. Displacement reconstructions by the phase unwrapping method based on this algorithm are experimentally validated, with laser subject to the moderate feedback regime.

OCIS codes: 120.2650, 280.3420, 120.0280.

doi: 10.3788/COL201311.091203.

As an emerging sensing technique, self-mixing interferometry (SMI) has attracted extensive research in the past two decades^[1]. SMI has practical advantages compared with standard interferometry; for example, the former does not require any optical parts external to laser chips and can be used in various measurements^[2]. SMI can also be applied in different scientific and industry applications; these include measurements of vibrations^[3–11], flow speed^[12–15], displacement^[1,16–20], and absolute distance^[21–23]. It can also be used to characterize laser parameters^[24–26].

A basic SMI structure consists of a laser diode (LD), a microlens, and a moving target, which forms an external LD cavity. With a small portion of light backscattered or reflected by the moving target reentering the LD cavity, the amplitude and frequency of LD power are modulated^[27]. The power is monitored through a photodiode (PD) enclosed in a typical LD package. At very weak optical feedback levels ($0 < C < 0.2$), the self-mixing (SM) signal is nearly a sine. At high injection levels ($0.2 < C < 1$), the interferometric waveform exhibits minor distortions caused by sinusoidal behavior. At moderate optical feedback ($1 < C < 4.6$), the waveform becomes sawtooth-like and exhibits hysteresis. The SM signal is converted into a fringe-free signal under the strong feedback regime.

The SM approach to displacement measurement is desirable because it is applicable to diffusers and untreated target surfaces, as well as serves as an alternative to the use of a corner cube. This approach is also considerably cheaper and simpler to operate. Literature indicates that displacement measurements are generally performed with laser subject to moderate feedback because this regime is the most commonly encountered during experiments^[17,28]; furthermore, it can readily provide the sign of displacement increments^[2]. Donati *et al.*^[28] developed a fringe counting method on the basis of the fact that each fringe on a SM waveform corresponded to a half-wavelength shift of a moving target. The method is simple but achieves the resolution of only a half wavelength for displacement measurement. In achieving high resolution, an attractive approach is the phase unwrapping method, which establishes unique mapping from the

SM waveform and the laser phase, after which it provides accurate displacement. Merlo *et al.*^[29] proposed a phase unwrapping method based on a SMI sensing model with a reconstruction accuracy of $\lambda_0/67$ on a scale of tens of nanometers. Despite the advantages of the approach, however, it entails time-consuming estimation of C and preliminary experimental calibration before the linewidth enhancement factor can be evaluated. Bes *et al.*^[17] presented a new reconstruction algorithm suitable for moderate feedback, and estimated the C value by using an optimization criterion based on the instantaneous power of reconstructed signal discontinuities. This approach is also time consuming^[8] and vulnerable to noise. Fan *et al.*^[1] improved the accuracy of SMI for displacement measurement by using an accurate feedback phase obtained through the accurate identification of four characteristic points and through an update of the C value on the basis of reconstructed signal discontinuities.

In the phase unwrapping method, a straightforward approach to retrieving target displacement from the SM signal involves two steps^[17]. The first is obtaining the feedback phase, and the second is determining the value of C and calculating the target displacement. The key point of the phase unwrapping method, therefore, is the detection of SM signal fringes. Each missed and/or false transition detection directly affects the accuracy of displacement measurement by a factor of $\lambda_0/2$. The SM signal is usually differentiated to extract switchings as pulses^[28]. In Ref. [17], a precalculated threshold value is used for transition detection, but this method works well only for a specified regime and may cause erroneous detection as soon as the SM regime changes or in the presence of noisy signals^[30]. Wavelet transform was then employed to improve the robustness of this detection method^[31]. Moreover, transition detection has been performed through computations of the Holder exponent with the use of differential evolution algorithms^[32]. This process differentiates the shapes of noisy signals, thereby enabling displacement recovery. Nevertheless, the approach involves very long computations. Zabit *et al.*^[8] proposed an algorithm that they improved by introducing the adaptive transition detection method, which could detect all SMI fringes by automatically converging to the

optimal threshold. The improved algorithm can work at weak and moderate feedback levels, but before the SM signal can be used, the algorithm needs a prefilter while the SM signal generated is noisy. Some filters can change positions for some characteristic points, such as the sharp transitions in a SM waveform^[33]. A technique based on “instantaneous” fringe-frequency determination was proposed to correctly detect speckle-affected SM fringes at a poor signal-to-noise ratio (SNR). This method is an intrinsic average process of computing fringe duration so that single spikes or signal losses do not significantly affect measurement^[4]. However, this method can be used only for vibration measurement when target vibration is sinusoidal.

This letter aims to correctly detect SM fringes at low SNRs and in the presence of disturbances without prefiltering. The detection is realized with the piece-wise transition detection algorithm.

The theory that governs SMI has been described by various authors and can be summarized as follows^[17,34]. Let $L(t)$ represent the instantaneous distance between a LD, which is generally driven by a constant injection current, and a remote target. When SM occurs, the laser wavelength is no longer the constant λ_0 but becomes a function of time $\lambda_F(t)$ under varying $L(t)$. Wavelength fluctuations can be found by solving the phase equation

$$x_0(t) = x_F(t) + C \sin[x_F(t) + \arctan(\alpha)], \quad (1)$$

where α is the linewidth enhancement factor that lies within the range^[3–10]. This interval corresponds to the extreme values taken by α for most of the LDs used in sensing applications^[35]. Figure 4 in Ref. [35] shows that large variations are not characteristic of α ; $x_F(t)$ and $x_0(t)$ represent two phase signals with and without optical feedback, expressed as

$$x_F(t) = 4\pi L(t)/\lambda_F(t), \quad (2)$$

$$x_0(t) = 4\pi L(t)/\lambda_0. \quad (3)$$

Optical output power fluctuation $P(t)$ is therefore given by

$$P(t) = P_0[1 + m \cos(x_F(t))] = P_0[1 + m \cdot g(t)], \quad (4)$$

where P_0 is the emitted optical power under free-running conditions, and m is the modulation index that depends on the reflection coefficient of the target^[36].

On the basis of Eq. (4), $x_F^r(t)$ is obtained by applying the inverse cosine function to $g(t)$; that is, $x_F^r(t) = \arccos[g(t)]$. The derivative of $x_F^r(t)$ is then compared with a threshold value to ascertain the presence of transition (or a fringe) through a transition detector. The value of the threshold level is critical for transition detection. With the need for a fully automated algorithm that converges to the optimum threshold level, the fringes can be correctly detected at a SM signal characterized by a good SNR (Fig. 1(a)). Under a noisy signal (e.g., electronic preamplifier noise and quantum noise associated with detected photons), however, the method causes errors in transition. It also causes a false reconstruction of displacement. Figure 1(b) shows that Gaussian white noise with a SNR of 16 dB is incorporated into the SM signal shown in Fig. 1(a). Two transitions are neglected

as shown by the red circle in Fig. 1(b).

Correctly detecting fringes from noisy SM signals necessitates improving the transition detection algorithm. The principle of the piece-wise transition detection algorithm is illustrated in Fig. 2.

Raw measurement data of about 5000 points, corresponding to several periods of target oscillation, are acquired. After the automatic gain control (AGC) of $P(t)$ is used to derive $g(t)$ ranging over $a \pm 1$ interval, an arc cosine function is employed to obtain $x_F^r(t)$. The derivative of $x_F^r(t)$, $\Delta x_F^r(t)$, is then evenly divided into several segments, such as k segments, which are expressed as $\Delta x_{F1}^r(t)$, $\Delta x_{F2}^r(t)$, \dots , $\Delta x_{Fi}^r(t)$, \dots , $\Delta x_{Fk}^r(t)$.

The transition of each segment is obtained by transition detection for segments (dotted box, Fig. 2). For the moderate feedback regime, the upper and lower halves of the SM signals (Fig. 1(a)) represent target displacement away and toward the LD, respectively. Therefore, the upper half of a hysteresis-affected SM signal ($P(t) > 0$) and the lower half ($P(t) < 0$) are separately treated to generate correct results. In the i th segment, the initial threshold value of the upper half is 15% of the maximum of $\Delta x_{Fi}^r(t)$. The initial threshold value of the lower half is 15% of the minimum of $\Delta x_{Fi}^r(t)$. That is, percent=0.15, where percent is the ratio of the threshold value to the maximum/minimum of $\Delta x_{Fi}^r(t)$. For a correct threshold value, only negative transitions should be obtained for

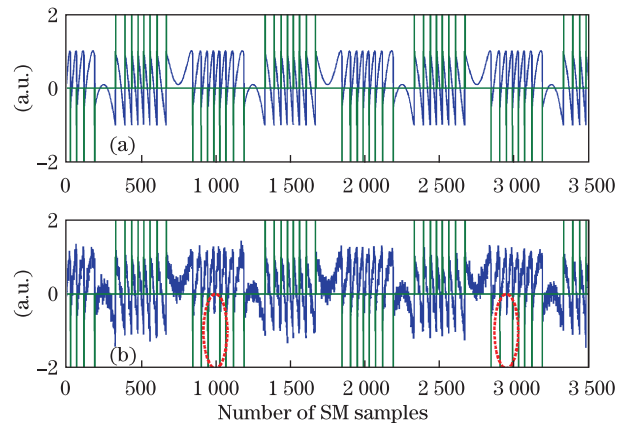


Fig. 1. (Color online) (a) Simulated SM signal with no noise (blue) and its correct transition detection (green), (b) a noisy SM signal (blue, SNR=16 dB) and its incorrect transition detection (green).

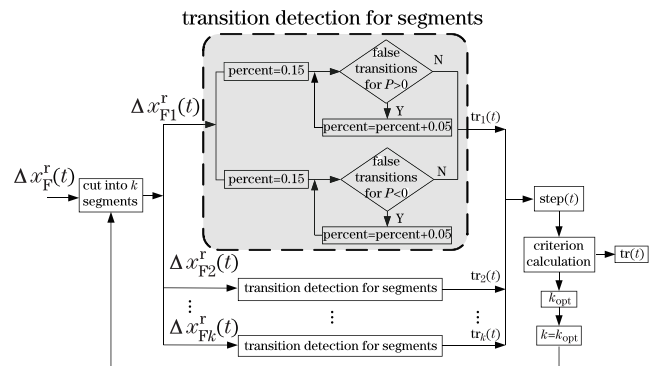


Fig. 2. Piece-wise transition detection algorithm.

the SM signal that corresponds to $P > 0$ ^[8]. If alternating positive and negative transitions are obtained for $P > 0$, then the threshold is too low. Consequently, the threshold is incremented by 5% of the maximum of $\Delta x_{F_i}^r(t)$. This loop continues until the threshold value becomes sufficiently large to rule out the possibility of false transition detection for the positive half of the SM signals in the moderate feedback regime. At $P < 0$, only positive transitions should be obtained. Therefore, the threshold is decremented by 5% of the minimum of $\Delta x_{F_i}^r(t)$ until the threshold value becomes small enough to rule out the possibility of false transition detection.

Then, all the transitions of each segment are connected. When considering harmonic signals, k_{opt} is derived through the optimization of a criterion $J(k)$ to estimate the optimal number of segments. This parameter is written as

$$\text{Argmin}(J(k)) = \text{Argmin} \sum_n \text{tr}(n), \quad (5)$$

where $\text{tr}(n)$, $n \in \mathbb{IN}$ is the discrete form of $\text{tr}(t)$, which is the detected transition of the SM signal. The criterion depends on the uniformity of target motion amplitude as harmonic target movement is considered.

As shown in Fig. 3, the transitions of the SM signal shown in Fig. 1(b) are correctly detected by the piece-wise transition detection algorithm. This newly presented transition detection algorithm, incorporated into phase unwrapping^[17], is used for displacement reconstruction. A maximum absolute error of less than 120 nm is observed for the SM signal, under an assumed LD of $\lambda_0 = 650$ nm.

The piece-wise transition detection algorithm has been theoretically validated for the variation of C from 1.0 to 4.6. The algorithm can correctly detect all SM fringes even at a low SNR of 16 dB.

Simulated sinusoidal signals and harmonic displacement signals have been correctly reconstructed by this algorithm. Figure 4 presents a triangular displacement signal, for which the vibrating amplitude is $3\lambda_0$ and the

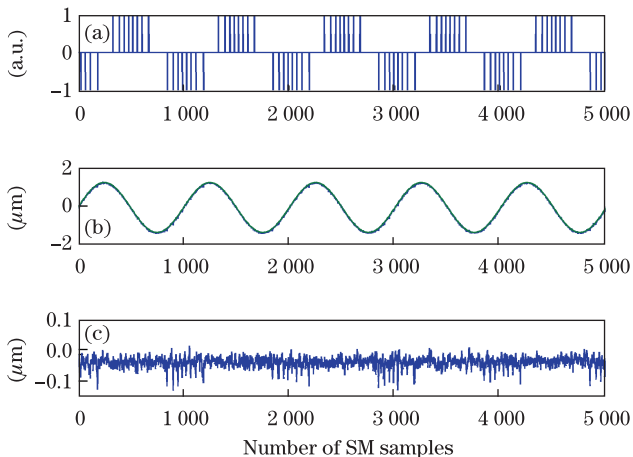


Fig. 3. (Color online) (a) Correct transition detection ($k_{\text{opt}}=3$), (b) displacement excitation (green) and its reconstruction (blue), and (c) the error generated by the excited and reconstructed signals.

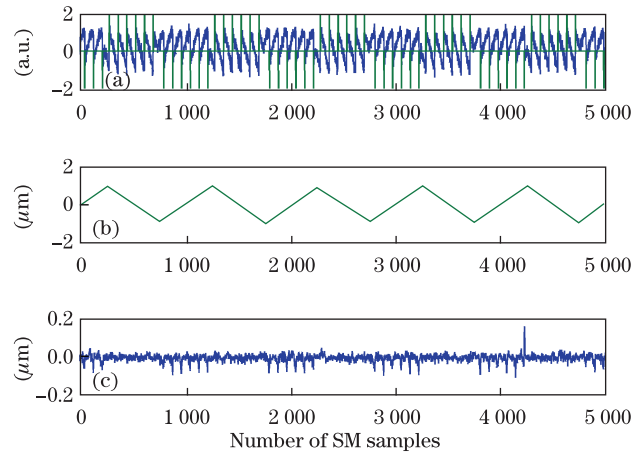


Fig. 4. (Color online) (a) Simulated SM signal and its correct transition detection ($k_{\text{opt}}=4$), (b) triangular displacement excitation (green) and its reconstruction (blue), and (c) the error generated by the excited and reconstructed signals.

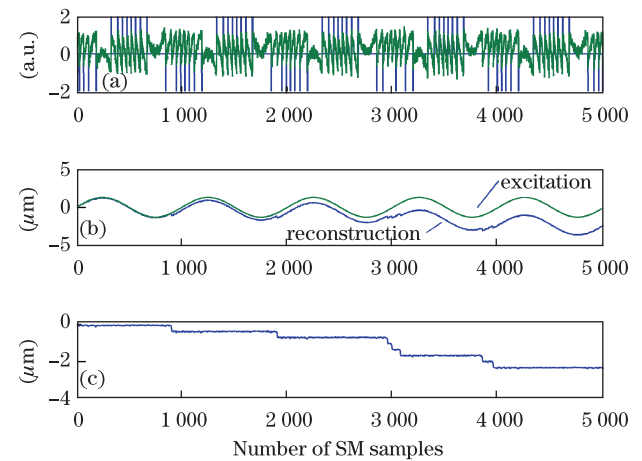


Fig. 5. (a) Very noisy simulated SM signal and its transition detection (SNR=15 dB), (b) displacement excitation and its reconstruction, and (c) the error generated by the excited and reconstructed signals.

SNR is 16 dB. The algorithm detects all the fringes in this signal, with a maximum absolute error of approximately $0.2\lambda_0$.

The proposed algorithm cannot correctly detect all fringes at low-quality SM signals, but it can detect transitions to minimize errors in displacement reconstruction. Figure 5 (SNR=15) indicates that the maximum absolute error generated by the traditional transition detection method is approximately $2.40 \mu\text{m}$. False/missed transitions are cumulative when the phase unwrapping method is used for displacement reconstruction. The phase unwrapping method supplies an incremental measurement of displacement. Accordingly, the measurement is incorrect if counting is lost because of transient signal dropout. Previous false/missed transitions cause drifting in the latter displacement reconstruction (Fig. 5(b)). However, the optimization of the criterion $J(k)$ depends on the minimum drift of an entire waveform. Optimization reduces the overall reconstruction error. The maximum absolute error is approximately 320 nm at an assumed LD of $\lambda_0 = 650$ nm (Fig. 6).

The proposed technique has also been verified with

experimental data. The experimental setup is shown in Fig. 7, which shows a metal plate fixed on a high-precision piezoelectric transducer (PZT, PI, P517.3 CD). The metal plate is used as the target. The proprietary capacitive sensor of the PZT directly measures position without physical contact at a resolution of 1 nm. The output of this sensor is used as the reference vibration amplitude (VA) measurement of actual target vibration amplitude. A low-cost, single-mode commercial LD (QL65D5SA, QSI Co., Korea) with a 650-nm wavelength is used for the SM sensor. This inexpensive laser source is not an ideal candidate for a SMI because it exhibits a low SNR under the SM effect. Most practical examples of SM instruments use near-infrared LDs with power levels of tens of milliwatts or distributed feedback LDs^[3,8]. The advantages of a low-power red LD are its low cost and good visibility for simple target aiming. Therefore, the proposed technique is implemented to overcome this noise problem. A variable attenuator is used to adjust the fraction of light backreflected into the LD optical cavity. The SM signal monitored by the PD in the LD package is sent through a transimpedance amplifier and then digitized with a data acquisition module (NI, USB6251).

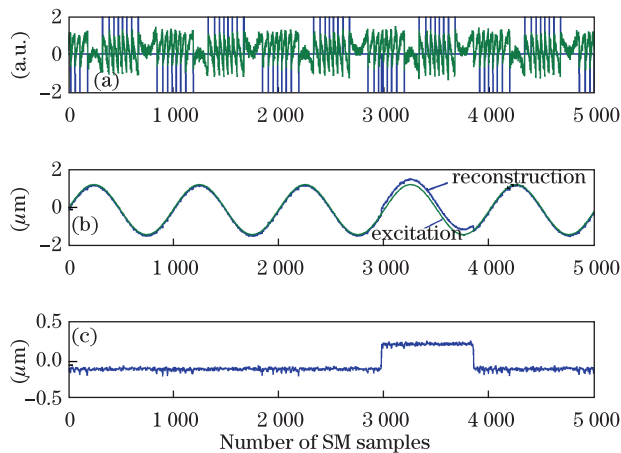


Fig. 6. (a) Transitions detected by the piece-wise transition detection algorithm (SNR=15 dB, $k_{\text{opt}}=3$), (b) displacement excitation and its reconstruction, and (c) the error generated by the excited and reconstructed signals.

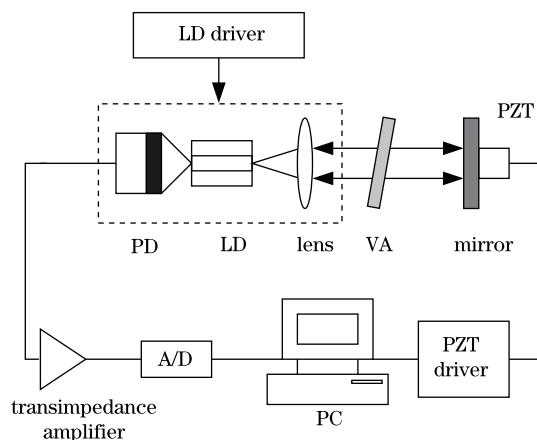


Fig. 7. Experimental setup.

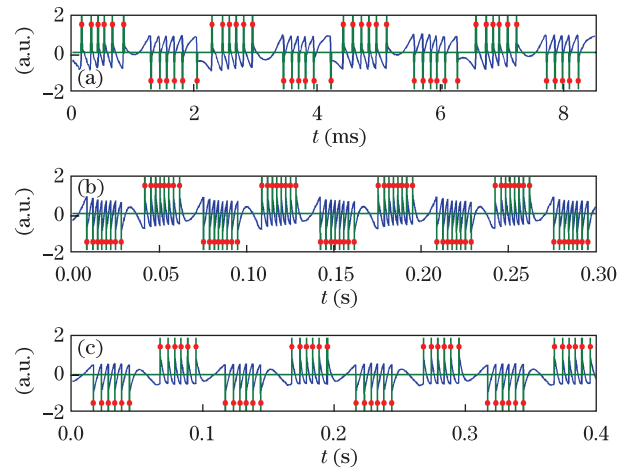


Fig. 8. (Color online) Experimental moderate feedback SM signals with good SNRs (blue), and correct detection of all SM fringes by the piece-wise transition detection algorithm (green line) and by the classic transition detection algorithm (red dot).

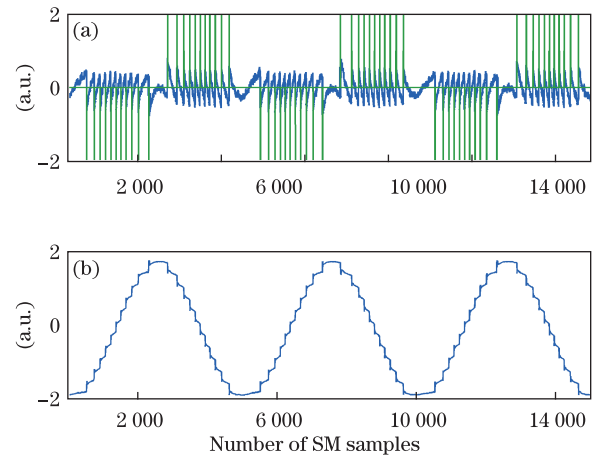


Fig. 9. (Color online) (a) Experimental moderate feedback SM signal (blue) and its transition detection (green) ($k_{\text{opt}}=3$), and (b) reconstructed displacement.

Figure 8 shows examples of signal processing for SM signals with good SNRs. The algorithm correctly detects all the fringes in these signals. For a good SNR, the results of the new algorithm are in optimum agreement with those derived by the classic transition detection algorithm.

For a poor SNR (Fig. 9), the moderate SM signal for p-p target displacement is $3.652 \mu\text{m}$ with a target modulation frequency of 10 Hz. All the SM fringes are again correctly detected without the need for filtering. Incorporating the algorithm into the phase unwrapping method yields a final error of less than 1% with respect to the reference PZT sensor. Using the same setup as the third case (Fig. 8(c)), another SM signal is acquired (Fig. 10(a)) for a target displacement of $1.71 \mu\text{m}$. Compared with the previous signal (Fig. 9(a)), this signal exhibits less hysteresis but a higher SNR. Nevertheless, the noise is unevenly distributed and mutations occur. The algorithm identifies all the transitions, thereby being able to reconstitute displacement with an error of 37 nm at its maxima with respect to the reference PZT sensor (Fig. 10(b)).

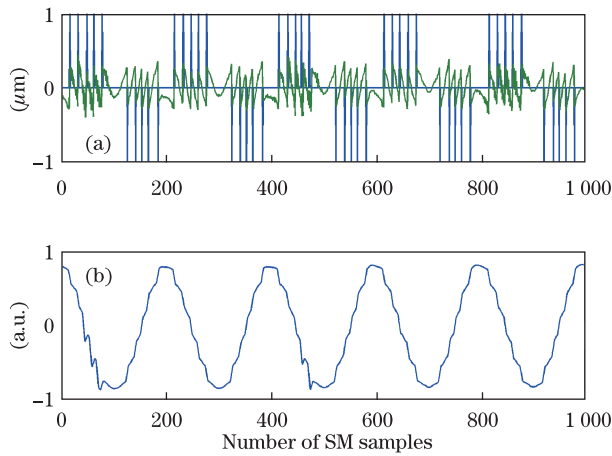


Fig. 10. (Color online) (a) Experimental moderate feedback SM signal with better SNR (green) and its transition detection (blue) ($k_{\text{opt}}=2$), and (b) reconstructed displacement.

In conclusion, we propose a technique for improving the measurement performance of a SM-based displacement sensing system. The desired improvement is achieved by using the proposed piece-wise transition detection algorithm, which correctly detects transitions from noisy SM signals without the need for prefiltering. The validity of the method is demonstrated through signal simulation and confirmed by several experimental measurements. This new method is also consistent with the classic transition detection algorithm when applied to interferometric signals of high quality (i.e., the same results are generated). The features of this algorithm enable the reduction of requirements for optical and electronic component use in interferometers, thereby facilitating the realization of high accuracy with simple and potentially very low-cost instrumentation.

This work was supported by the Natural Science Foundation of Heilongjiang Province under Grant No. F201105. The authors would also like to thank Profs. Jiwen Cui and Yuhang Wang (Center of Ultra-Precision Optoelectronic Instrument, Harbin Institute of Technology) for their assistance in the experiments.

References

1. Y. Fan, Y. Yu, J. Xi, and J. F. Chicharo, *Appl. Opt.* **50**, 5064 (2011).
2. S. Donati, *Laser Photon. Rev.* **6**, 393 (2012).
3. G. Giuliani, S. Bozzi-Pietra, and S. Donati, *Meas. Sci. Technol.* **14**, 24 (2003).
4. M. Norgia and C. Svelto, *IEEE Trans. Instrum. Meas.* **57**, 1703 (2008).
5. S. Donati, M. Norgia, and G. Giuliani, *Appl. Opt.* **45**, 7264 (2006).
6. M. Norgia, A. Pesatori, M. Tanelli, and M. Lovera, *IEEE Trans. Instrum. Meas.* **59**, 1368 (2010).
7. P. A. Roos, M. Stephens, and C. E. Wieman, *Appl. Opt.* **35**, 6754 (1996).
8. U. Zabit, T. Bosch, and F. Bony, *IEEE Sens. J.* **9**, 1879 (2009).
9. C. Li, Z. Huang, and X. Sun, *Chin. Opt. Lett.* **11**, 21201 (2013).
10. L. Lu, J. Yang, L. Zhai, R. Wang, Z. Cao, and B. Yu, *Opt. Express* **20**, 8598 (2012).
11. L. Lu, Z. Cao, J. Dai, F. Xu, and B. Yu, *IEEE Photon. Technol. Lett.* **24**, 392 (2012).
12. M. Norgia, A. Pesatori, and L. Rovati, *IEEE Trans. Instrum. Meas.* **59**, 1233 (2010).
13. M. H. Koelink, F. F. M. De Mul, A. L. Weijers, J. Greve, R. Graaff, A. C. M. Dassel, and J. G. Aarnoudse, *Appl. Opt.* **33**, 5628 (1994).
14. S. K. Ozdemir, S. Takamiya, S. Ito, S. Shinohara, and H. Yoshida, *IEEE Trans. Instrum. Meas.* **49**, 1029 (2000).
15. M. Norgia, A. Pesatori, and L. Rovati, *IEEE Sens. J.* **12**, 552 (2012).
16. M. Norgia, S. Donati, and D. D'Alessandro, *IEEE J. Quantum Electron.* **37**, 800 (2001).
17. C. Bes, G. Plantier, and T. Bosch, *IEEE Trans. Instrum. Meas.* **55**, 1101 (2006).
18. M. Norgia and S. Donati, *IEEE Trans. Instrum. Meas.* **52**, 1765 (2003).
19. M. Wang and G. Lai, *Rev. Sci. Instrum.* **72**, 3440 (2001).
20. Z. Zeng, S. Zhang, S. Zhu, W. Chen, and Y. Li, *Chin. Opt. Lett.* **10**, 121404 (2012).
21. M. Norgia, G. Giuliani, and S. Donati, *IEEE Trans. Instrum. Meas.* **56**, 1894 (2007).
22. M. Norgia, A. Magnani, and A. Pesatori, *Rev. Sci. Instrum.* **83**, 045113 (2012).
23. S. Kakuma and R. Ohba, *Opt. Rev.* **10**, 511 (2003).
24. Y. Yu, J. Xi, and J. F. Chicharo, *Opt. Express* **19**, 9582 (2011).
25. Y. Yu, G. Giuliani, and S. Donati, *IEEE Photon. Technol. Lett.* **16**, 990 (2004).
26. M. Fathi and S. Donati, *IET Optoelectronics* **6**, 7 (2012).
27. S. Donati, *J. Appl. Phys.* **49**, 495 (1978).
28. S. Donati, G. Giuliani, and S. Merlo, *IEEE J. Quantum Electron.* **31**, 113 (1995).
29. S. Merlo and S. Donati, *IEEE J. Quantum Electron.* **33**, 527 (1997).
30. G. Plantier, C. Bes, T. Bosch, and F. Bony, in *Proceedings of IEEE Conference on Instrumentation and Measurement Technology* 1013 (2005).
31. C. Bès, T. Bosch, G. Plantier, and F. Bony, *Opt. Eng.* **45**, 084402 (2006).
32. A. Doncescu, C. Bes, and T. Bosch, in *Proceedings of IEEE Conference on Sensors* 382 (2007).
33. Y. Sun, Y. Yu, and J. Xi, *Proc. SPIE* **8351**, 83510G (2012).
34. R. Lang and K. Kobayashi, *IEEE J. Quantum Electron.* **QE-16**, 347 (1980).
35. G. Plantier, C. Bes, and T. Bosch, *IEEE J. Quantum Electron.* **41**, 1157 (2005).
36. T. Bosch, N. Servagent, and M. Lescure, in *Proceedings of IEEE Conference on Instrumentation and Measurement Technology* 870 (1997).